

INTEGRITY ASSESSMENT OF CRACKED COMPONENTS USING PROBABILISTIC METHODS

I. Varfolomeyev¹, O. Yasniy²

¹*Fraunhofer IWM, Freiburg, Germany*

²*National University of Lviv, Ukraine*

Abstract. In this study probabilistic methods of the fracture mechanics are applied to integrity assessment of cracked components subjected to static and cyclic loading. Various key issues related to a probabilistic analysis are discussed and accounted for in the calculations. An example illustrating the application of computational procedures to evaluate the integrity of a component with postulated cracks is presented. Finally, some available experimental results on fatigue crack growth are re-evaluated based on the use of statistical methods.

Introduction

Fracture mechanics assessment of components containing existing or postulated flaws is usually performed based on deterministic approaches. These act on proper assumptions of the flaw state, material strength and toughness properties, as well as applied loading. Generally, deterministic estimates of component's strength are conservative, provided that state-of-the-art analysis methods together with reliable and conservative input data are employed. However, many applications deal with variable or/and uncertain data whose impact on the final result cannot be distinctly judged. If appropriate, uncertainties and scatter in the input parameters are taken into account by applying sensitivity studies or using certain percentile curves to describe material properties (e.g. within the 90% confidence interval).

Alternatively, methods of statistical data analysis and probabilistic fracture mechanics can be applied. In this case, available measurements of material properties, load magnitudes and sequences, and results of the non-destructive evaluation (NDE) can be directly involved in the analysis as statistically distributed quantities. An essential advantage of such an approach is that the critical conditions (e.g. crack size, loading, material toughness) or the component life-time can be expressed in form of distribution functions, so that both the expectation (median value) and the scatter of the sought solution parameter can readily be quantified.

A considerable progress in the probabilistic fracture mechanics methods achieved within past two decades was mainly due to research activities on component safety and damage tolerance in nuclear and conventional power plants, aerospace, pipeline, pressure vessel industries. Numerous examples of the probabilistic assessment of cracked components are considered in the literature, e.g. [1-4]; several computer programs and benchmark results are available [5-6]. Moreover, probabilistic methods are included in the latest versions of the structural integrity assessment procedures [7-9].

Although the general solution approach in the probabilistic fracture mechanics analysis is well established, several computational issues need to be systematically considered. In particular, the following topics should be addressed:

- methods of the data fit using various distribution functions;
- evaluation of the fit accuracy and validity criteria for distribution assumptions;
- statistical description of random data, such as applied loading in fatigue problems, and their extrapolation (e.g. in the time domain);
- random data generation;
- calculation of probabilistic integrals and failure probabilities;
- evaluation of the scatter in the final results.

Associated computational methods and mathematical algorithms, as well as related fracture mechanics models and solutions are briefly reviewed in this paper. Subsequently, probabilistic analyses are performed to evaluate fracture probabilities in a piping containing

postulated defects [9]. Furthermore, available crack growth data for surface cracked plates in cyclic bending [10] are re-evaluated using probabilistic analysis tools.

Analytical Failure Assessment

Failure assessment procedures, e.g. [7-9], accepted for the use in industrial applications employ the failure assessment diagram (FAD) for components under static loading and elastic stress intensity factor solutions for predicting fatigue crack growth under cyclic loading.

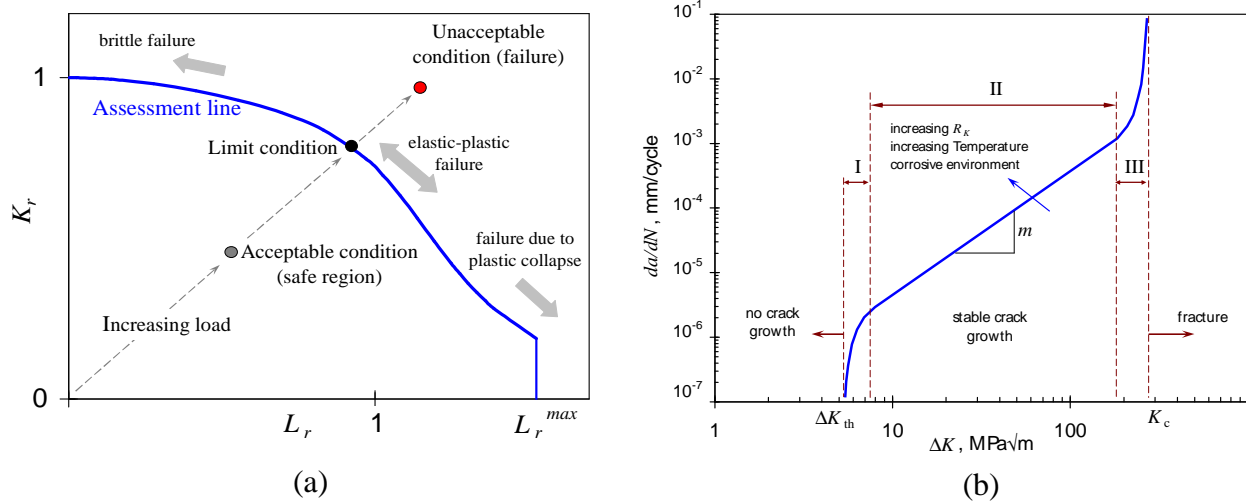


Fig. 1. Typical FAD (a) and fatigue crack growth curve (b) for a cracked component.

Figure 1 schematically illustrates both approaches and related analysis methods. The assessment point in FAD is defined by [7]

$$K_r = \frac{K_{Ip}}{K_{mat}} + \frac{K_{Is}}{K_{mat}} + \rho, \quad L_r = \frac{P}{P_L} = \frac{\sigma_{ref}}{\sigma_Y} \quad (1)$$

with K_{Ip} and K_{Is} being elastic stress intensity factors for the primary and secondary loading, respectively, K_{mat} the material fracture toughness, ρ a plasticity correction accounting for the interaction between the primary and secondary stresses, P (or σ_{ref}) a measure of the primary load, and P_L (or the yield strength σ_Y) the load (respectively, stress level) corresponding to the yielding of the cracked ligament. The failure assessment line, $K_r = f(L_r)$, separating the safe state region from that assigned to the component failure (Fig. 1a) is determined based on the tensile data available (yield strength, ultimate strength, stress-strain curve) [7].

Calculations of fatigue crack propagation are generally performed assuming a material specific relationship between the crack growth rate, da/dN , and the stress intensity factor range, ΔK . In a simple case of constant amplitude loading, the Paris-Erdogan equation applies (region II in Fig. 1b):

$$\frac{da}{dN} = C \Delta K^m \quad (2)$$

Deterministic failure assessment is based on conservative assumptions of the material data (strength properties, fracture toughness, fatigue crack growth rates and threshold value, ΔK_{th}), crack size (e.g. above accepted NDE limits) and location, as well as the load magnitude. Moreover, considerable conservative simplifications of the load spectrum are often performed in fatigue calculations. An additional use of safety factors [7-9] aims at providing sufficient safety margins for problems involving scattering or uncertain data. In general, this leads to a considerable underestimation of the critical conditions (load, defect size) and life-time for a cracked component, so that a further data refinement may become necessary to prove the component safety.

On the other hand, the above approach is not able to completely exclude the risk of failure. For instance, the scatter in material properties cannot be entirely captured by specimen

testing, so that severe data variations about the expected values are possible. Furthermore, even though long-term load measurements are available for certain components, extreme loads can still arise. In such cases, methods of statistical analysis and probabilistic fracture mechanics are able to improve and supplement the deterministic analysis and provide more realistic predictions of component behaviour.

Significance and Description of Data Scatter

Input data involved in fracture mechanics calculations can be separated in three groups: geometry, material and loading. Most or even all of the input parameters are subjected to the variability and uncertainty which causes the variability of the final solution. To describe the scatter in the input data and account for this in the analysis, methods of the mathematical statistics and probability theory are employed.

The table below summarises some distribution functions used in technical application.

Table 1. Typical distribution functions employed in engineering calculations.

Distribution type	Distribution parameters	Probability density function	Eq.
Normal	μ = mean σ = standard deviation $-\infty < x < \infty, \sigma > 0$	$f(x) = \frac{1}{\sigma\sqrt{2\pi}} \exp\left[-\frac{1}{2}\left(\frac{x-\mu}{\sigma}\right)^2\right]$	(3)
Lognormal	x_0 = location parameter m = scale parameter σ = shape parameter $x_0 \leq x < \infty, m > 0, \sigma > 0$	$f(x) = \frac{1}{(x-x_0)\sigma\sqrt{2\pi}} \exp\left[-\frac{1}{2\sigma^2}\left(\ln\frac{x-x_0}{m}\right)^2\right]$	(4)
Weibull	x_0 = location parameter β = shape parameter η = scale parameter $x_0 \leq x < \infty, \eta > 0, \beta > 0$	$f(x) = \frac{\beta}{\eta} \left(\frac{x-x_0}{\eta}\right)^{\beta-1} \exp\left[-\left(\frac{x-x_0}{\eta}\right)^\beta\right]$	(5)
Exponential	b = scale parameter x_0 = location parameter $x_0 \leq x < \infty, b > 0$	$f(x) = \frac{1}{b} \exp\left[-\frac{(x-x_0)}{b}\right]$	(6)

A statistical description of the flaw state includes two key aspects: (1) flaw size distribution; (2) probability of detection (POD) of a crack having a certain size a . The flaw size distribution depends both on material quality and NDE requirements. The lognormal and exponential distribution functions, Eqs (4), (6), are suitable for describing the initial crack size. The probability of detection is related to the amount of NDE data and the quality of employed apparatus.

The material is characterised by its strength and fracture mechanics parameters. The scatter in the yield and tensile strength can often be described by fitting available test results to normal or lognormal distribution functions, Eqs (3)-(4). A considerable scatter of the fracture toughness, especially in the brittle-to-ductile transition region, is a critical point to be accounted for in the analysis of cracked components. An appropriate statistical description of fracture toughness is achieved using a three-parameter Weibull distribution, Eq. (5), of the master curve method [11]. Various statistical approaches are known to treat the scatter of fatigue crack growth data [1, 2].

To account for uncertainties and variability of the applied load, different procedures are used [1-6]. Fatigue analyses additionally employ methods for counting measured load spectra. Furthermore, statistically based extrapolation techniques have been developed [12].

Failure probabilities or fatigue crack growth calculations are often performed making use of the Monte-Carlo simulation (MCS). However, this method becomes rather inefficient if low failure probabilities are requested. In such cases, the first- or second-order reliability methods (FORM, SORM) [13], as well as MCS with importance sampling [14] are advantageous.

Examples of Probabilistic Assessment

The following two examples illustrate the performance and potentials of probabilistic methods in the assessment of cracked components under both static and cyclic loading.

Component under static loading

This example deals with strength and burst safety assessment of a spiral welded pipe made of steel StE480.7TM (API X70) [9]. Imperfections in the welds have originated when the welded, finished and pressure tested pipes were turned on support rollers to put on the outer insulation under heating. As a consequence of malfunctions of the support rollers, the weld metal area was locally deformed leading to the cold forming and reduction of material toughness in the weld areas [9, 15].

The imperfections are located between the weld metal and heat affected zone and extend over about 200 mm parallel to the seam which is at an angle of 22° with the circumferential direction. By extensive hardness measurements, the cold formed zone was found to extend to a maximum depth of 2 mm into the pipe wall. To exclude the pipe failure, the whole cold formed zone is conservatively assumed to be a long surface crack of the depth $a = 2$ mm. The static internal pressure is $p = 7.6$ MPa. Additionally, residual weld stresses (secondary stresses) of magnitude $\sigma_s = 0.6R_{p0.2}$ are imposed on the structure; this assumption is conservative, since the residual stresses are likely to disappear in the cold formed area.

Figure 2 summarises the component and crack geometry, load parameters and material data and shows the model employed in calculations. The fracture toughness was estimated based on measurements of the crack tip opening displacement; hereby, the smallest of 10 individual values ($\delta_c = 0.05$ mm) was used [15].

Table 2 presents distribution functions and related parameters employed in the probabilistic analysis. In particular, the fracture toughness is assumed to follow a three-parameter Weibull distribution according to the master curve concept, whereas the value of $K_{mat} = 91$ MPa \sqrt{m} is assigned to the failure probability of 5%. To explore the significance of the crack depth assumptions, two mean values $\mu_a = 2$ and 3 mm are analysed.

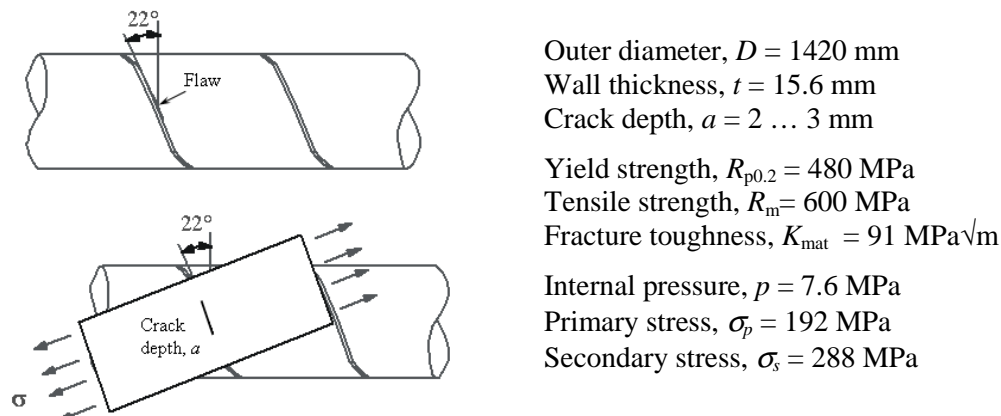


Fig. 2. Geometry of the spiral welded pipe and respective analysis model.

Table 2. Data for probabilistic assessment of the spiral welded pipe.

Input data	Mean value	Distribution type	Distribution parameters
Crack depth a , mm	2	normal	$\mu = 2, \sigma = 0,2$
	3		$\mu = 3, \sigma = 0,3$
Primary stress σ_p , MPa	192	normal	$\mu = 192, \sigma = 4$
Secondary stress σ_s , MPa	288	lognormal	$x_0 = 282, m = 6, \sigma = 0,6$
Yield strength $R_{p0,2}$, MPa	480	lognormal	$x_0 = 474, m = 6, \sigma = 0,4$
Tensile strength R_m , MPa	600	normal	$\mu = 600, \sigma = 10$
Fracture toughness K_{mat} , MPa \sqrt{m}	91	Weibull	$x_0 = 20, \beta = 4, \eta = 149$

Probabilistic calculations are first performed using MCS with the total number of simulations varied between $N = 10^3$ and 10^6 . The failure probability is then determined by

$$P_f = N_f / N \tag{7}$$

where N_f is the number of failure cases, as predicted according to the FAD approach, Eq. (1). Figure 3 shows the analysis results obtained at $N = 10^3$. Here a unique assessment line corresponding to the mean values of the material strength and toughness parameters is drawn; the assessment points are scaled according to their position in the diagram at each individual simulation with randomly selected input data (Table 2). The failure probability is $P_f = 0.004$ for the mean crack depth of $\mu_a = 2$ mm and $P_f = 0.026$ for $\mu_a = 3$ mm. With increasing number of simulations, the result tends to $P_f = 4.08 \times 10^{-3}$ for $\mu_a = 2$ mm and $P_f = 3.05 \times 10^{-2}$ for $\mu_a = 3$ mm.

The failure cases occasionally predicted in Fig. 3 are mainly due to low values of the fracture toughness, as derived from the presumed Weibull distribution with the lower bound of $K_{min} = 20$ MPa \sqrt{m} . While this assumption is generally too conservative, further analyses are carried out to specify the minimum required fracture toughness needed to assure a certain reliability level of the piping. A target failure probability of 7×10^{-5} is selected, as requested for non-redundant components with severe failure consequences [7]. Failure probabilities calculated by the second-order reliability method are given in Fig. 4 as a function of the lower bound of fracture toughness. The results suggest that the values $K_{min} = 47$ and 82 MPa \sqrt{m} would provide the desired reliability level for the piping with the mean crack depth of 2 and 3 mm, respectively. Hence, comprehensive measurements of the fracture toughness, as well as a reliable non-destructive examination are two decisive actions to assure a safe operation of the piping.

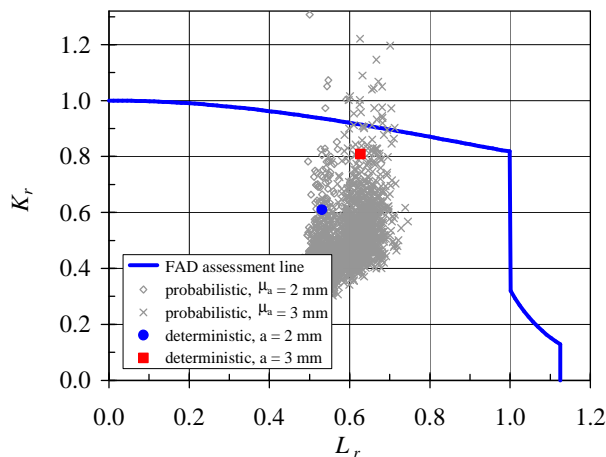


Fig. 3. Probabilistic FAD assessment of the spiral welded pipe.

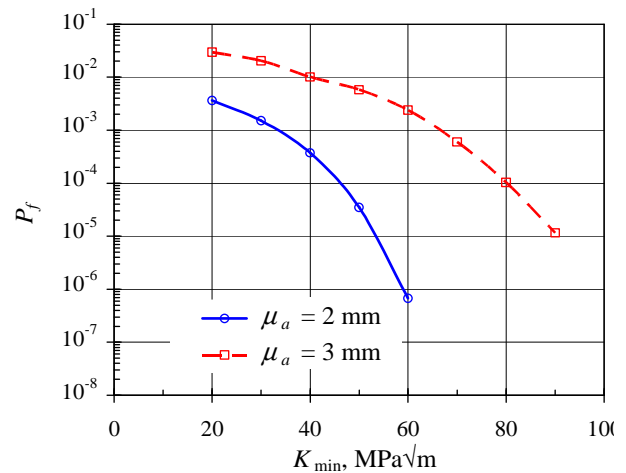


Fig. 4. Failure probability versus the lower bound of fracture toughness.

Assessment of fatigue crack growth

In [10], experimental results are presented for surface cracked specimens made of steel 15X2MΦA, subjected to cyclic bending with the stress ratio $R = 0.32$. Analytical calculations of fatigue crack growth were performed on the deterministic basis within the Paris region of the fatigue crack growth curve, Eq. (2), using the constants $C = 2.96 \times 10^{-8}$, $m = 2.54$ (da/dN in mm/cycle, ΔK in $\text{MPa}\sqrt{\text{m}}$), Fig. 5. In particular, predicted fatigue lives for specimens with semi-elliptical cracks were within 30% of the experimental results.

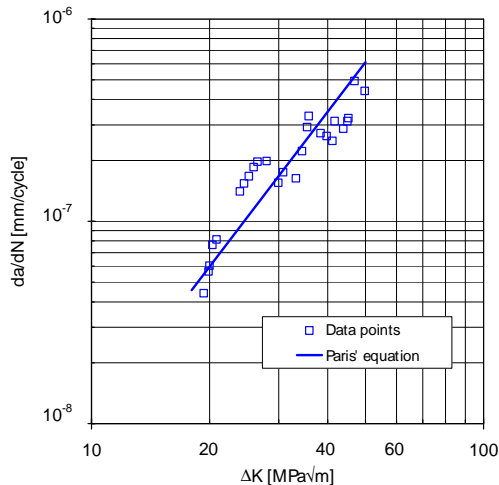


Fig. 5. Fatigue crack growth data for steel 15X2MΦA, $R = 0.32$ [10].

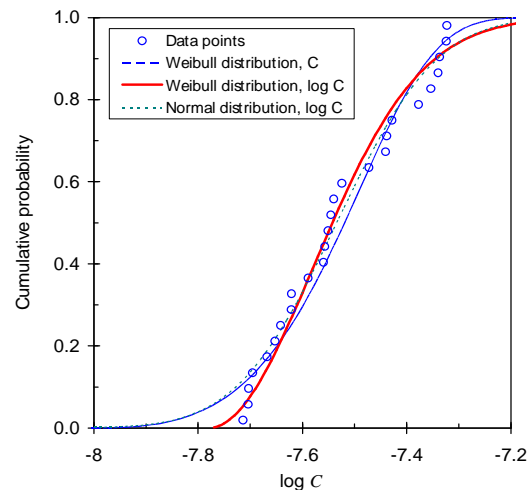


Fig. 6. Distribution functions for the parameter C in Eq. (2), $m = 2.54$.

In this example, probabilistic analysis is applied to evaluate the significance of the data scatter in Fig. 5 and to derive distribution functions for fatigue lives of the corresponding specimens.

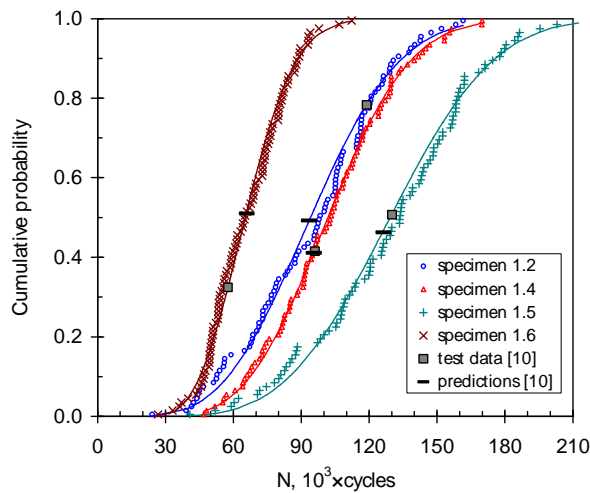
Since the Paris constants C and m are often considered to be dependent parameters, a common approach to describe the scatter of FCG data is to fix one of them and vary the other one [1]. Assuming $m = 2.54$, the cumulative distribution function for C or $\log C$ can be derived, Fig. 6. This was fitted using the normal, lognormal and Weibull distribution functions, Eqs (3)-(5), both for C and $\log C$. Subsequently applying the Anderson-Darling goodness-of-fit (AD-GOF) test, only three distributions were found to be acceptable, Fig. 6. The solid line in Fig. 6 provides the best fit to the empirical data and is described by equation

$$F(\log C) = 1 - \exp\left[-\left(\frac{\log C + 7.78}{0.286}\right)^{1.983}\right] \quad (8)$$

The value $C = 2.96 \times 10^{-8}$ employed in [10] corresponds to the probability of some 54%.

Using randomly generated values of C , crack growth analyses for four specimens (designation 1.2, 1.4, 1.5, 1.6) tested in [10] were performed by integrating Eq. (2). For each specimen, 100 simulations were completed. Figure 7 summarises the input data and analysis results in terms of the cumulative probability function for fatigue lives.

An appropriate analytical description of the empirical data is achieved by applying the Weibull distribution for either N or $\log N$, as well as the normal distribution for $\log N$. However, the AD-GOF test succeeded for all data sets only when using the Weibull distribution for $\log N$, as shown by solid lines in Fig. 7.



Specimen: plate with a semi-elliptical surface crack

Plate thickness: 30 mm, width: 116 mm

Loading: cyclic bending, $R = 0.32$

a_0 : initial crack depth

$2c_0$: initial crack length

a_f : final crack depth

N : number of cycles in test

Specimen	1.2	1.4	1.5	1.6
σ_{\max} , MPa	366	454	395	471
a_0 , mm	8.8	3.9	5.4	6.0
$2c_0$, mm	25.2	12.4	12.2	13.4
a_f , mm	17.7	18.6	18.3	16.1
N , cycles	119000	96100	130200	57700

Fig. 7. Fatigue life distributions of surface cracked specimens under cyclic bending.

Deterministic fatigue life predictions obtained in [10] correspond with the probability level of 41% to 51%, as expected for the mean curve in Fig. 5; the experimental results cover the probability range of 32% to 78% (Fig. 7).

Conclusions

Probabilistic methods are a valuable extension to conventional (deterministic) analysis tools, allowing for consideration and handling of uncertainties, variability and scatter in the input parameters. On one hand, probabilistic calculations help to quantify the influence of individual parameters and their scatter on the final result; on the other hand, they provide estimates of component's limit state or life-time in terms of probability distribution functions. The latter brings essential advantages over the deterministic approach, e.g. in explaining occasional failure cases of components whose design is believed to be safe. Moreover, probabilistic calculations can be efficiently used to specify requirements on the input data in order to reach a targeted reliability level, as shown in the first example of the paper.

Results of a probabilistic analysis are reliable and, thus, valuable provided that accurate and statistically representative input data are involved. In particular, the use of underlying distribution functions must be carefully checked. As discussed in the last example of the paper, wrong assumptions on the type of distribution functions can be eliminated by properly applying goodness-of-fit tests. Finally, adequate methods for computing failure probabilities should be employed. Specifically, calculations of low failure probabilities require accurate algorithms based on the FORM or SORM.

References

1. Bloom, J.M., Ekvall, J.C. (Eds.), Probabilistic Fracture Mechanics and Fatigue Methods: Applications for Structural Design and Maintenance, ASTM STP 798, American Society for Testing and Materials (1983).
2. Provan, J.W. (Ed.), Probabilistic Fracture Mechanics and Reliability, Martinus Nijhoff Publ. (1987).
3. Cioclov, D., Kröning, M., Probabilistic fracture mechanics approach to pressure vessel reliability evaluation, in *Probabilistic and Environmental Aspects of Fracture and Fatigue*, ASME PVP Vol. **386**, pp. 115-125 (1999).
4. Rahman, S., Kim, J.S., Probabilistic fracture mechanics for nonlinear structures, *Int. J. Pressure Vessels and Piping* **78**, 261-269 (2001).
5. Dillström, P., ProSINTAP – A probabilistic program implementing the SINTAP assessment procedure, *Eng. Fracture Mechanics* **67**, 647-668 (2000).

6. Brickstad, B., Dillström, P., Schimpfke, T., Cueto-Felgueroso, C., Chapman, O.J.V., Bell, C.D., Project NURBIM (nuclear RI-ISI methodology for passive components), benchmarking of structural reliability models and associated software, in *Flaw Evaluation, Service Experience, and Materials for Hydrogen Service*, ASME PVP Vol. **475**, pp. 109-119 (2004).
7. SINTAP: Structural Integrity Assessment Procedures for European Industry, Report BE 95-1426 (1999).
8. FITNET: Fitness-for-Service Procedure, Prepared by European Fitness-for-Service Thematic Network, M. Kocak et al., Eds. (2006).
9. Berger, C., Blauel, J.G., Hodulak, L., Pyttel, B., Varfolomeyev, I., Fracture Mechanics Proof of Strength of Engineering Components, FKM-Guideline, 3rd extended edition, VDMA Publ. GmbH (2006).
10. Varfolomeyev, I.V., Vainshtok, V.A., Krasowsky, A.Ya., Prediction of part-through crack growth under cyclic loading, *Eng. Fracture Mechanics* **40**, 1007-1022 (1991).
11. Wallin, K., The scatter in K_{Ic} results, *Eng. Fracture Mechanics* **19**, 1085-1093 (1984).
12. Socie, D., Modelling expected service usage from short-term loading measurements, *Int. J. Materials & Product Technology* **16**, 295-303 (2001).
13. Der Kiureghian, A., De Stefano, M., Efficient algorithm for second-order reliability analysis, *J. Engineering Mechanics* **117**, 2904-2923 (1991).
14. Engelund S., Rackwitz R., A benchmark study on importance sampling techniques in structural reliability, *Structural Safety* **12**, 255-276 (1993).
15. Bernasovski P., Lombardini J., Cracking of SAW welds in gas pipelines, in Proc. Pipeline Conference, Oostende, November 1990, pp. 13.19-13.24 (1990).